



# Modelling the Effect of Geometry and Loading on Mechanical Response of SARS-CoV-2

Diplesh Gautam<sup>1</sup> · Nizam Ahmed<sup>1</sup> · Venkatesh KP Rao<sup>1</sup>

Accepted: 14 May 2022 / Published online: 14 June 2022

© The Author(s), under exclusive licence to Springer Science+Business Media, LLC, part of Springer Nature 2022

## Abstract

In recent times, coronavirus (SARS-CoV-2) becomes a pandemic disease across the globe. This virus affects the severe acute respiratory system that causes a type of pneumonia, which results in an outbreak in Wuhan, China, and then in whole global countries. The virus possesses a complex structure and varied in composition along with its geometrical shape and size. Contributions of the lipid and protein components of a virus to the influenza viral envelope's mechanical properties are still unknown. In this work, the virus is modeled like the SARS-CoV-2 and surrounded with spikes made up of S glycoproteins, and numerical analysis was made to predict its mechanical behavior while resting on the substrate. The static and viscoelastic response of the virus was carried out in a finite element (FE) commercial software Ansys. The impact of changing viral envelope thickness on SARS-CoV-2 and bald virus stiffness was investigated. The viscoelastic analysis shows the increase in the deformation and stress with an increase in the pressure. The static analysis predicts the lower stiffness for SARS-CoV-2 compared to bald virion and increases with the increase in the envelop thickness. This study is useful for analyzing the effect of geometry and mechanical properties on the mechanical response of SARS-CoV-2.

**Keywords** SARS-Cov-2 · Stiffness · Elastic modulus · Numerical modelling · Viscoelastic

## 1 Introduction

Coronaviruses belong to a family of viruses that inspire respiratory illness in people, including the primary cold and progressively severe diseases [1], for example, Middle East respiratory syndrome (MERS) and severe acute respiratory syndrome (SARS). This gathering of infectious viruses can cause zoonotic transfer to human, as was shown during the situation for MERS and SARS outbreaks. A few member of other species, for example, bats, behaved as repositories for conveying wide assortments of viruses, and epidemic viral outbreak in the human population [27]. SARS and MERS transmitted from other species to the human because of their close contact. The novel coronavirus (as of now alluded to

as 2019-nCoV) was first identified in Wuhan, China, in December 2019 and appeared to infect the individuals who had visited an open seafood animal market [14]; also, the individual-to-individual spreading of viruses took place very rapidly which cause severe respiratory diseases and lead to death in many cases. Studies on the source of 2019-nCoV are effectively ongoing, and information about its transmissibility and incubation period is continuously developing. Chemistry plays a vital role in understanding each component of the viral structure and its pathogenesis [8]. It helps Researchers, Virologists, and Clinicians to improve the materials and techniques for identifying vaccine and treatment of an epidemic disease. It is necessary to understand the molecules that control the structure of viruses and its function for the development of means to cure infectious disease [22]. The coronavirus's current outbreak illustrates the critical nature of basic science and the need for continuous research based on the available resources.

### 1.1 Structure and Mechanism of Viral Infection

Researchers moved quickly to characterize and describe 2019-nCoV and disseminate their findings among the global

✉ Diplesh Gautam  
p20180436@pilani.bits-pilani.ac.in

Nizam Ahmed  
nizam.ahmed@pilani.bits-pilani.ac.in

Venkatesh KP Rao  
venkateshkp.rao@pilani.bits-pilani.ac.in

<sup>1</sup> Department of Mechanical Engineering, BITS Pilani, Pilani 333031, Rajasthan, India

research community as fast as possible under these epidemic circumstances. Mathematical modeling and dynamics of a novel coronavirus (2019-nCoV) were described to the cause of infection and considered the seafood market of Wuhan china as originated place, and fractional model was used for infection minimization [15]. A significant study on homology models of the novel coronavirus cysteine protease was described and predicted the fast accessibility of 2019-nCoV genomic information and the creation of first-generation homology models for 3CL<sup>pro</sup> cysteine protease; a compound which helped in viral replication and investigated as an objective for antiviral treatments in the treatment of coronavirus, like SARS [39]. This proposed that the viral genome bears a nearby similitude to bat coronaviruses. The protease shows the nearest homology with SARS-CoV protease a zoonotic infection virus that entered the human population through civets. The coronavirus spike protein is a multi-functional molecular machine that mediates coronavirus entry into host cells [7]. It first binds to a receptor on the host cell surface through its S1 subunit and then fuses viral and host membranes through its S2 subunit. Two domains in S1 from different coronaviruses recognize various host receptors, leading to the viral attachment. The spike protein exists in two structurally distinct conformations, prefusion and postfusion. The transition from prefusion to the postfusion conformation of the spike protein must be triggered, leading to membrane fusion. The structures and functions of coronavirus spike proteins, describing the two S1 domains by recognizing different receptors and the role of spike proteins in the conformational transitions phase. A comparative study of coronavirus spike proteins, receptor recognition, and membrane fusion functions in the context of the corresponding functions from other viruses and host cells was proposed [36]. Viruses are nano-sized structures. During extracellular transmission, the virus genome is protected by their shells, generally protein capsid and lipid envelope from being damaged. Protein capsids are having minimalistic and pose asymmetric structure. The domain of a membrane protein that extended into the extracellular space is an ectodomain. Membrane proteins are typical proteins that form part of biological membranes, or interact with them. This simple structure is enough for the protection of their genome, viral infection, and replication. For possessing these roles, shells must be strong and softer against applied pressure, mechanical straining, and environmental condition, such as temperature [12]. The mechanical studies of viral structure will help to explain the organization of the viral shells, their responses to changes in the environment, and the relation between the viral mechanics and viral functions in their life cycle. There are various experimental techniques available on the mechanical behavior of the viruses. The osmotic shock method was used to determine the strengthening phenomenon of the bacterial

microphages [33]. Brillouin light-scattering was used to examine the mechanics of virus crystal [38]. This technique helps to gain the direction-dependent average behavior of the large-size particles. Optical tweezers are another method used to study biological viruses and cells. Biological cells are kept between two beads. In which one bead bound to a DNA molecule and another bead to a microphages pro head and was trapped by laser beams. By approaching the beads, motion, and forces of DNA by the viral motor was recorded by the optical tweezers. [30] [37]. Optical microscopy can also be used to measure forces and displacements that can be deduced from the diffracted laser beam from the trapped beads [9]. Atomic force microscopy (AFM) is one of the technique used for imaging and direct probing a single virus. In an AFM technique, the sample is probed with a sharp tip and imaged with a high resolution of a few nano meters in liquid. Protein surface and its structure organization on the virus's outer envelope can be clearly imaged by AFM, [4, 19, 20]. Its capability is not only for imaging but also for the analysis of the viruses. Falvo et al. was first to investigate the tobacco mosaic virus (TMV) with an AFM and predicted the mechanical behavior and properties of TMV while rotating, dissecting, and translating by an AFM tip [6] and the axial Young's modulus of the virus was reported. Later mechanical properties of viruses were evaluated from the force deformation curve obtained by applying point force indentation on the biological samples by the AFM tip [12]. Later on, the method has been applied to study various types of biological samples with or without envelope [12, 18, 29, 34, 35]. Sample stiffness was evaluated using these techniques for virus and further converted to material properties like Young's modulus using mechanical modeling. This mechanical modelling helps to understand the mechanical contribution of viral protein shell of the whole virus structure. The Young's moduli of enveloped and nonenveloped viruses were found to be in the range of up to 2.8 GPa [28]. The AFM technique is used to investigate the material properties of the viral shell and their contribution in strength to rest structure. Although Experimental techniques like AFM are used to observe the complex structure and integrity of the virus to obtain clear images and investigate the topography of the virus structure [26]. This technique was used to visualize crown-like virions and geometrical measurements of protein capsid mounted over the membrane envelope. This study revealed the characterization of the surface of SARS-CoV-2 particles at the nanoscale and offers new prospects for evaluating surface properties of the virus. The aim of this study is to investigate the mechanical behavior of a single native SARS-CoV-2 virus. We used a simplified model of virus in the CAD software. Lipids and glycoproteins spikes are considered in the model to address their contribution in the mechanical behavior of SARS-CoV-2. We investigated the impact of pressure on SARS-CoV-2 with changes in elastic support stiffness

using viscoelastic behavior. SARS-CoV-2 was compared to bald virions (formed on removing the glycoproteins spike from the surface of SARS-CoV-2) with varied geometrical and mechanical properties based on their static behavior.

## 2 Materials and Methods

Coronaviruses are massive large round particles with extended spike surface projections, as shown in Fig. 1. For the geometrical modeling of SARS-CoV-2, we considered the average diameter of the virus particles around 100 nm, and the length of the spike of 20 nm long situated over the outer envelope with 1–2 nm as an ectodomain part lying inside the envelope (similar dimensions mentioned in Steffen Klein et al. [17]). The infectious virus envelope in electron microscopy shows up as a distinctive pair of electron-dense

shells. The viral envelope comprises a lipid bilayer where the membrane film (M), envelope (E), and spike (S) and essential structural proteins are tied down and anchored. A subset of coronaviruses (explicitly the individuals from betacoronavirus subgroup A) have a shorter spike-like surface protein called hemagglutinin esterase (HE). Inside the envelope, the nucleocapsid is made from different duplicates of the nucleocapsid (N) protein, which are bound to the positive-sense single-stranded RNA genome in a long string form with continuous beads type configuration. The lipid bilayer envelope, layer proteins, and nucleocapsid ensure the virus outside the host cell. For the representation of the RNA core and lipid bilayer, we considered it as a thin spherical shell. The RNP core (ribonucleoproteins and RNA) generally consists of the virus’s genomic structure and nuclear capsids lying inside the lipid envelop. A novel coronavirus was modeled and its configuration is shown in Fig. 2.

**Fig. 1** **a** A cartoon model of SARS-CoV-2 virus with their various constituent parts and geometrical parameters. **b** Boundary conditions on a single virus particle with and without spike protein at the surface of a substrate during compression [21][25]

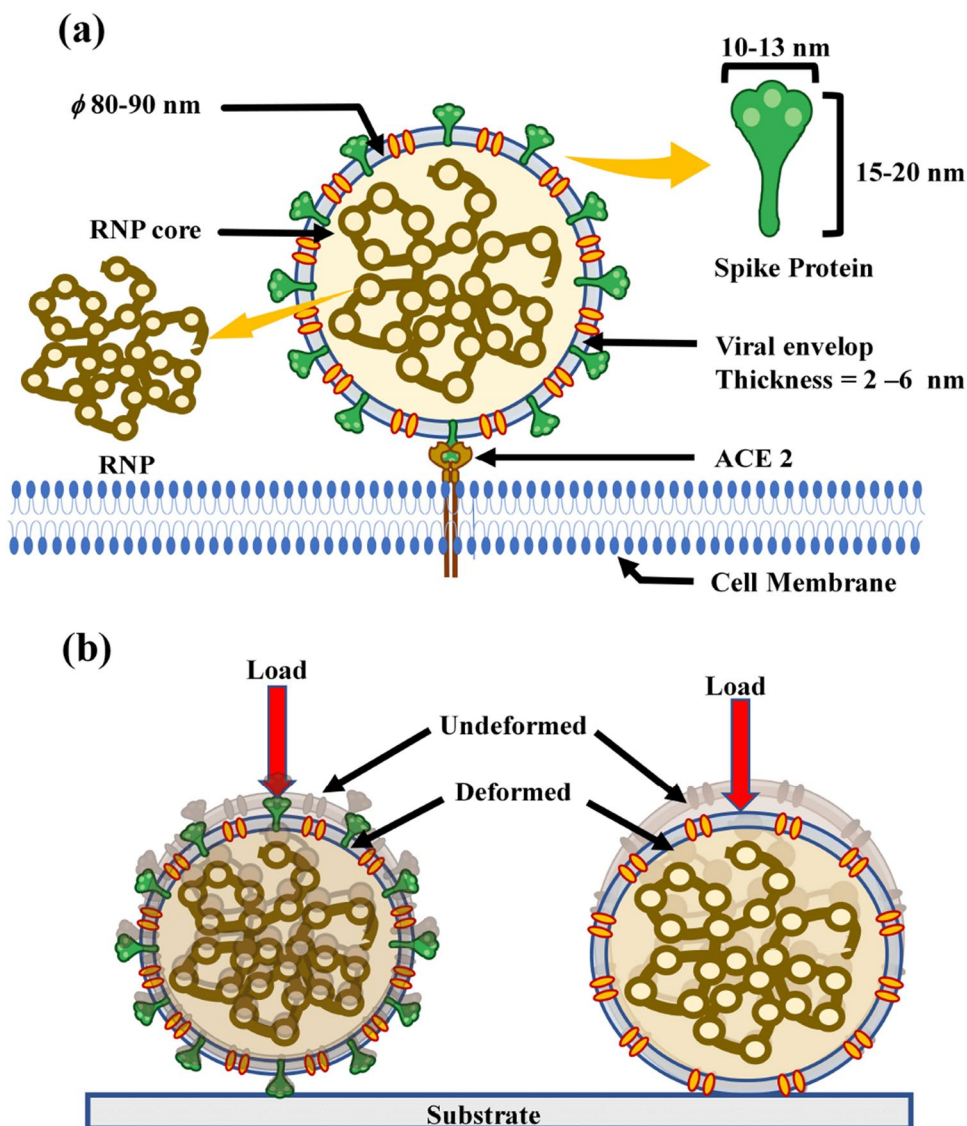
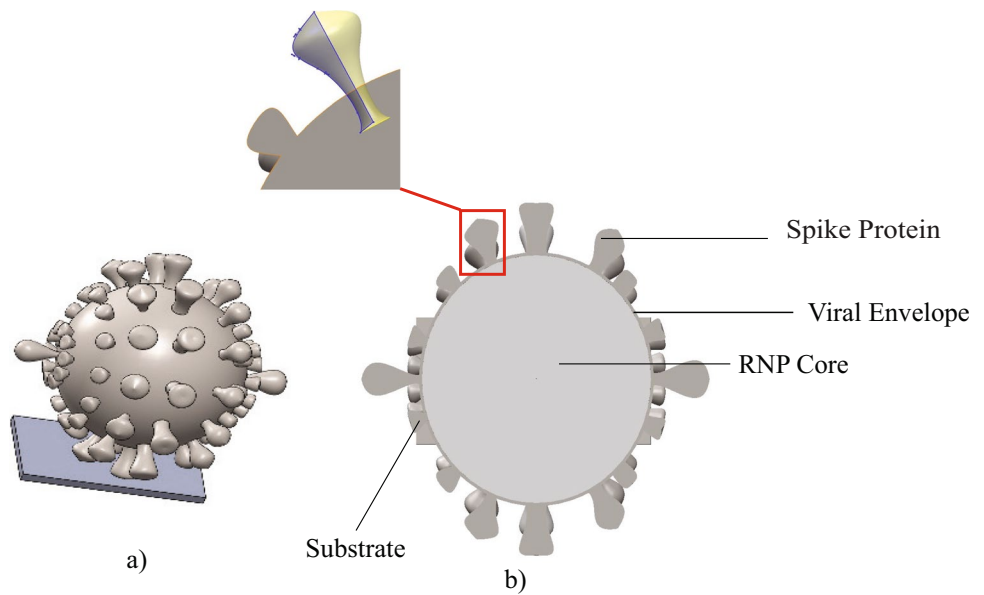


**Fig. 2** **a** Geometric model for SARS-CoV-2. **b** Sectional view of model



The main component of virus is proteases that respond to the transmission and invoke the new virus. Double dumbbell shape spike protein modeled to represent the same feature and behavior as the spike protein in the ideal coronavirus. The RNA and DNA part of the virus is represented as the spherical part of the virus. Dimensions of the various parts of the modeled geometry are shown in Table 1. In this work, the real phenomenon of force impact on the coronavirus lying on the substrate has done using structural analysis. Figure 1b shows the related boundary conditions during the compression of the SARS-CoV and bald virus. Also, the viscoelastic behavior of the coronavirus was modeled considering prony relaxation method.

A 3D modeled geometry is similar to that of novel coronavirus, which is antiological agents of SARS observed from the previous studies. The 100 nm diameter virus consists of all significant components that identified and contributing to the mechanics and cell conformation. It includes the mechanical properties of envelope, spike glycoprotein, M protein, hemagglutinin esterase dimer, lipid envelop, and RNP core [23] (Fig. 2). The three-dimensional geometry was created in SolidWorks™ software and exported to finite element package ANSYS. The spike protein and envelope play a critical role in defining the shape of the cell. Spike glycoprotein and M protein which are extended surface over the envelope are equally spaced and identical throughout the spherical surface conformation. Material properties assigned to the different virions constitute are shown in Table 1 (based on primarily peer-reviewed research). We have considered the Poisson's ratio of virus as 0.49 during the analysis [32].

## 2.1 Mathematical Formulation

Finite element modelling is one of the most important mathematical tool to analyze any complex structure. In the finite element modelling, discretization and assembling are the initial steps. In this study, the biological structure is discretized in tetrahedral elements and then assembled at nodes. Different type of elements and complex shape with rigorous loads and complex boundary conditions can be done together using finite element modelling. In this study, we kept the bottom rectangular substrate as zero displacement boundary condition and the compressive load of 1 nN was applied on the virus along the transverse direction. The finite element formulation initiates with the basic principle of variational total potential energy [16]. Using hookes law equation  $\sigma = \epsilon E$  and strain-displacement relation

$\epsilon = Bu$ , variation of the functional equation can be written as shown in Eq. 1.

$$\delta u^T \left[ \int_V B^T D B dV \right] u - \delta u^T \int_{sf} N t dS = 0 \quad (1)$$

Where  $N$  is matrix of shape functions. Equation 1 is the basic equation for the finite element discretization and can be converted to algebraic equations as follows  $Ku = f$ , where  $K$  is the element stiffness matrix,  $f$  is the vector  $R$  load. This equation system can be solved for unknown displacement vector  $u$  using any commercial Finite element software ANSYS, which includes a nonlinear and linear elements, material laws ranging from metal to rubber, with wide variety of available boundary conditions with high effective solvers. complex assemblies with different behavior of



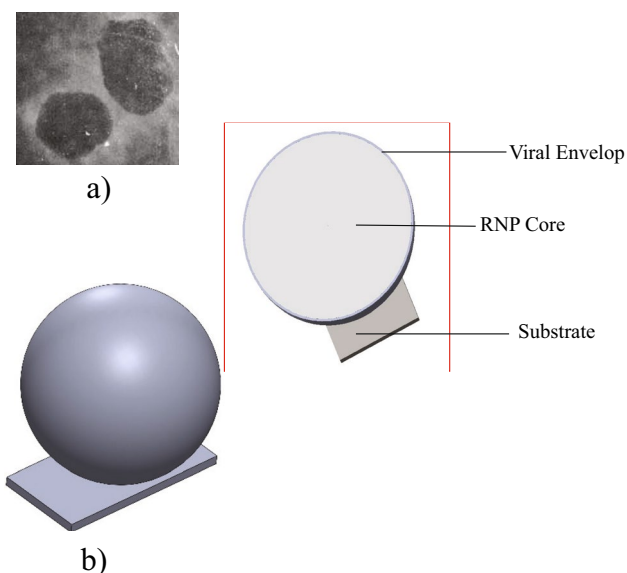


**Fig. 3** a Negative stain electron micrograph of bald virions [36]. b Geometric Model for bald virions with its constitutive parts (insets)

structure is the ideal choice for determining stresses, strain, frequencies, temperatures, displacements and contact pressure distributions on any part of geometry and assembly.

### 2.2 Viscoelastic Modeling

Viscoelasticity is the property of materials that possess both viscous and elastic behavior when undergoing deformation. Viscous materials generally resist shear flow with time when stress is applied, while elastic materials strained on the application of stress and immediately return to their original state on the removal of stress. Amorphous polymers, biopolymers, and even the living tissue and cells are the viscoelastic materials that are often modeled to determine their force and displacement relations. There are various models, such as the Maxwell model, the Kelvin-Voigt model, the standard linear solid model, prony model, and the Burgers model used to predict a material’s response under different loading conditions. For this study, we use prony viscous model because this model predicts the main effects of contact between the viscoelastic time scale of substrate’s and the

inter cellular time scale and helps to recognize the influence of various mechanical parameters [10]. In this model, material is subjected to a strain and kept constant over the period of time, and the stress is measured. The material’s elastic response indicates the initial stress in the material. For the different applied loading condition, notation for tensile-compressive relaxation is denoted by elastic modulus (E). For the prony shear relaxation method, the model is shown in Eq. 2.

$$G(t) = G_{\infty} + \sum_{i=1}^n G_i e^{-\frac{t}{\tau_i}} \tag{2}$$

Where shear modulus is denoted as G and t is a relaxation time. These constant values are shown in Table 1. Coronavirus modeled as a viscoelastic assigned by a neo-Hookean material, which is generally considered for the biological specimens. Prony shear relaxation method is used with a relaxation time of 1 s as shown in Eq. 2. For the analysis, the COVID-19 virus-cell kept over the substrate along with its spike proteins. 3D rectangular plate geometry is considered for the representation of the substrate. The pressure is applied over the top of the spike surface, and resting spike over the substrate is considered as the elastic support and the substrate considered as the zero displacement boundary.

### 2.3 Spike and Bald Virions

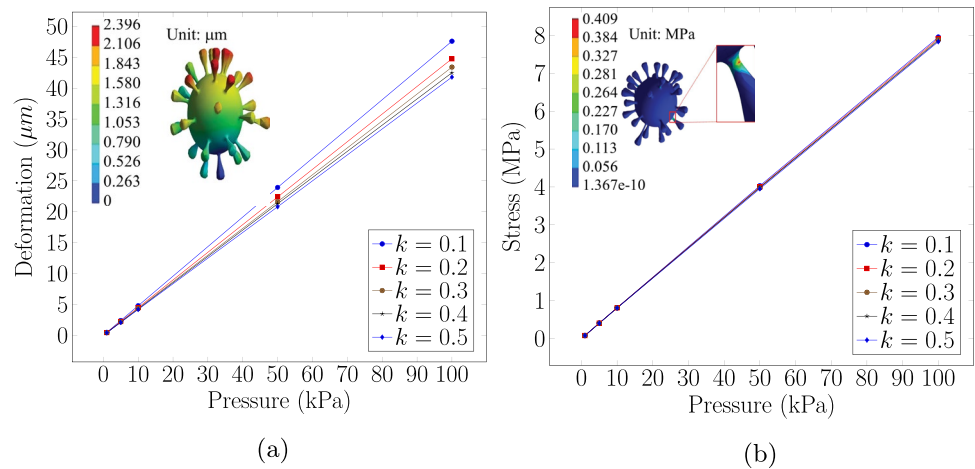
Spike virions are the virus having spike-shaped protruding structures over the outer envelope of the virus. Spike is connected through the intermediate layer, generally known as a lipid bilayer, and protruded outside the outer envelope of few nm in size. These spikes are glycoproteins that help to transmit the virus when interacted with the neighbor virus particles.

The ectodomain of the glycoproteins and spike proteins was removed from the surface to model the bald virions. Experimentally, bromelain treatment was used to remove protruded spikes, and hence the viral particle surface appeared smooth as shown in Fig. 3a. For the numerical analysis, spherical geometry is modeled without the spike parts representing bald virus (Fig. 3b). [36].

**Table 1** Geometric and on mechanical properties of the virions [2, 13, 24, 31]

Part	Constitute Parts	Dimension (nm)	Youngs Modulus (GPa)	Shear Modulus (GPa)
Spike protein	S glycoproteins	$l \approx 10-20$	3.5	1.175
Viral Envelop	Lipid bilayer and membrane proteins	$w \approx 2-6$	2.5	0.85
RNP core	Nucleocapsid protein and virial RNA	$d \approx 80-90$	2.0	0.65

**Fig. 4** **a** Effect of pressure variation on deformation at different elastic support stiffness. **b** Effect of pressure variation on Vonmises stress at different elastic support stiffness. Deformation (inset (a)) and Vonmises stress distribution (inset (b)) in COVID-19 for pressure 0.005 MPa and elastic support stiffness 0.1



### 3 Results

#### 3.1 Visco Elastic Modeling

COVID-19 was considered as a viscoelastic material for the analysis. Finite element analysis was done to predict the interaction of COVID-19 virus with the substrate. In this work, variation in the applied pressure ranges from few 1 Pa to 0.1 MPa and corresponding variation in elastic support and its effect on elastic stiffness observed and plotted in the graph shown in Fig. 4a and b.

From Fig. 4a, the deformation is varying linearly and increases on increasing the pressure. While increasing the elastic support, stiffness deformation decreases. This decrease in deformation is due to an increase in the virus particle strength while increasing the elastic stiffness of the virus. Similarly, the Von Mises Stress developed in the virus,

as shown in Fig. 4b and increases with the pressure and decreases with an increase in elastic stiffness.

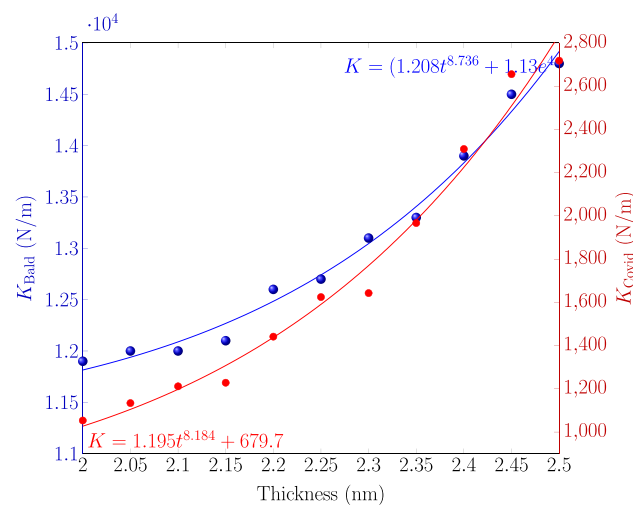


**Fig. 5** Stiffness comparison for bald virus and covid-19

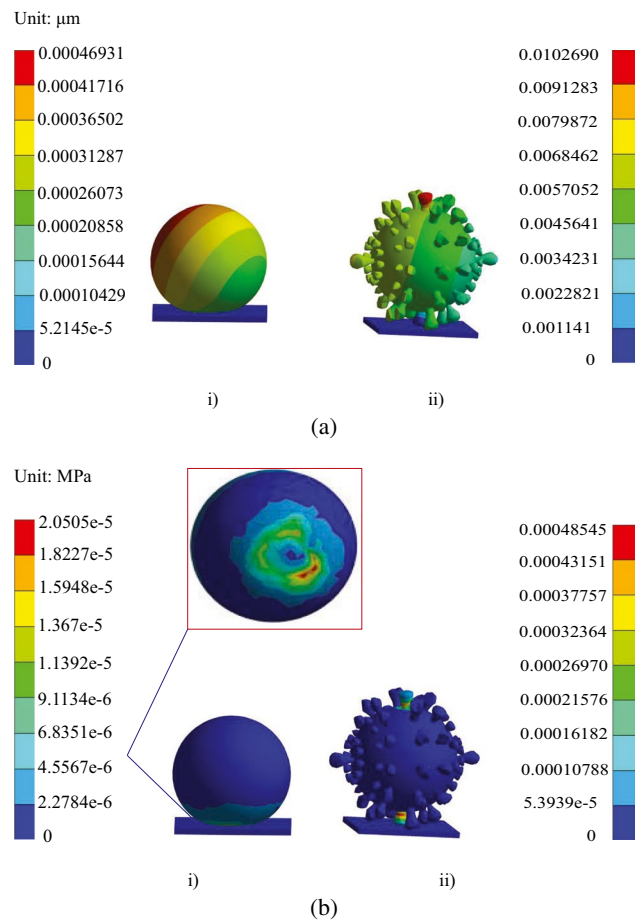


**Fig. 6** **a** Contour map for deformation variation (i) for bald virions and (ii) for COVID-19. **b** Contour map for stress variation (i) for bald virions and (ii) for COVID-19

### 3.2 Spike Glycoproteins are Contributing to the Stiffness of the Viral Envelope

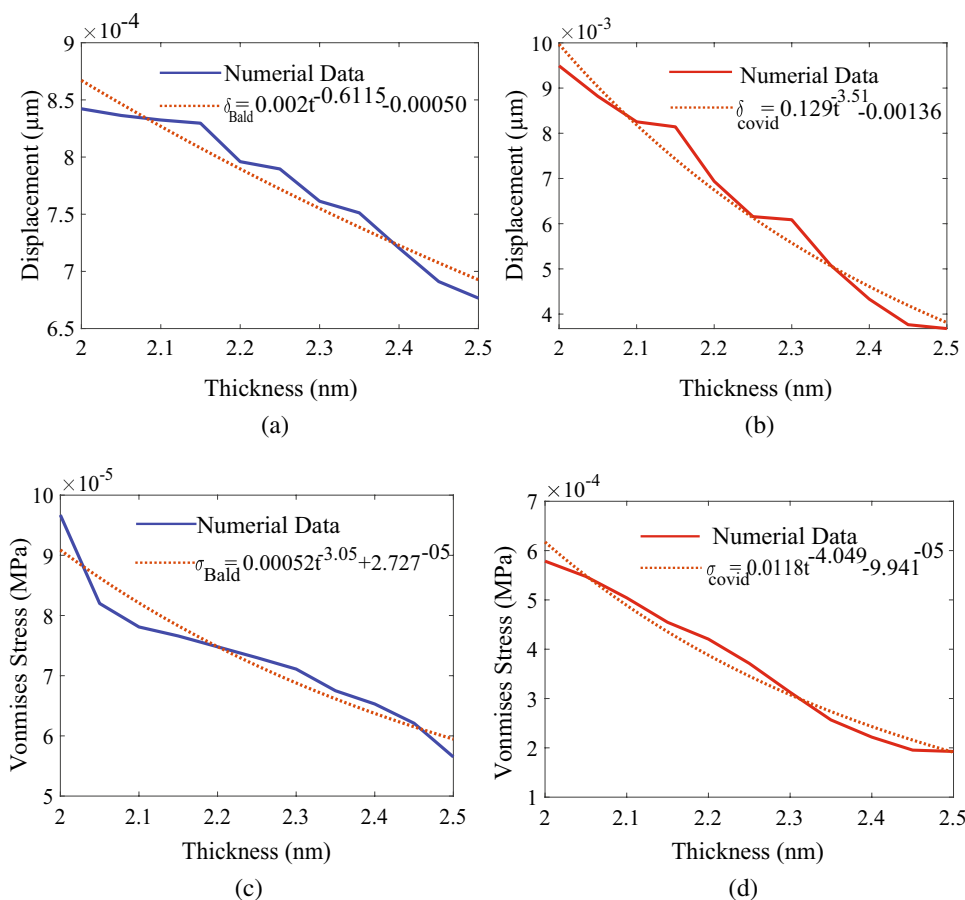
The force-displacement curves for the Covid-19 and bald virions obtained from a varying force applied on the virus model ranging from 1 nN to 100 nN with the fixed support boundary condition to the Substrate. From the obtained curve, the stiffness was evaluated. The stiffness measurements show the soft, linear phase of the force-displacement curves that were observed for both the virus, i.e., COVID-19 and the bald virions. At all forces, the response of bald virions was elastic and higher stiffness compared to the COVID-19 (Fig. 5). Figure 5 shows the stiffness for bald and COVID-19. It is observed that the stiffness for bald is 10–12 times that of the spike protruded COVID-19.

### 3.3 Change in Stiffness with Particle Size

We investigated the relationship between the stiffness of the virus and virus membrane size. Virus membrane size changed by varying the aspect ratio of the individual particle. The aspect ratio of the viral membrane changed with the change in membrane thickness. The stiffness at the different

thickness of the membrane evaluated, and the relation was given by the equation shown in Fig. 5. Plot for stiffness and thickness for virus model were obtained under the compressive force of 10 nN. The stiffness  $K$  was related to the thickness  $t$  of the particles, with  $K \approx t^n$ , as expected for spherical shells with thickness  $t$ . From Fig. 5, the stiffness increases as an increase in the thickness of membrane in bald virions from 2 nm to 2.5 nm. The predicted stiffness of the virions is about  $11900 \mu\text{N}/\mu\text{m}$ . While for COVID-19, total deformation of  $0.94 \text{ nm}$  with the total stiffness of  $1053.42 \mu\text{N}/\mu\text{m}$ . The contour plots for the deformation and stress distribution in the bald and COVID-19 are shown in Fig. 6a and b. Contour plot shows the maximum stress at the mating part of the Substrate and virus in the case of bald, while for the COVID-19 virus, it is at the narrow portion of the spike protein. We also investigated the effect of change in the membrane thickness on the deformation and vonmises stress. Figure 7 shows decrease in the deformation for both bald, as well as COVID-19. Similarly, decreases in vonmises stress. This decrease in deformation and stresses is occurred due to an increase in the strength and mass of the virus, which may lead to the known relation of stress directly proportional to strain.

**Fig. 7** Effect of change in viral membrane thickness on **a** deformation for bald virion, **b** deformation for COVID-19 virion, **c** Vonmises stress for bald virion, and **d** Vonmises stress for COVID-19 virion



### 3.4 Effect of Change in Viral Envelop Young's Modulus

Change in viral envelop Young's modulus affects the stiffness of the bald virions and COVID-19. Figure 8a shows an exponential decay in the deformation up to 8 MPa and further increase in elastic modulus, increases deformation for the bald virion. Initially increase in the elastic modulus of the envelop leads to a decrease in deformation. This shows the strengthening of the bald virus. Further increase in Young's modulus contributes to an increase in the strength of the structure of the virus but comparatively less than the initial increase. While in the case of COVID-19, results show an increase in the strength of the COVID-19 structure with the exponential decrease in the deformation because increase in Young's modulus of viral envelop as well as spike protein strength both are contributing to the strengthening of COVID-19 structure and it is sufficient to withstand the applied load. Figure 8b shows an exponential decrease in the stress with the increase in Young's modulus of the bald virions and COVID-19. There is an effect of change in Young's modulus of the viral envelop in the stiffness. As the deformation decreases, an increase in stiffness up to 8 MPa was observed, a further decrease in the stiffness.

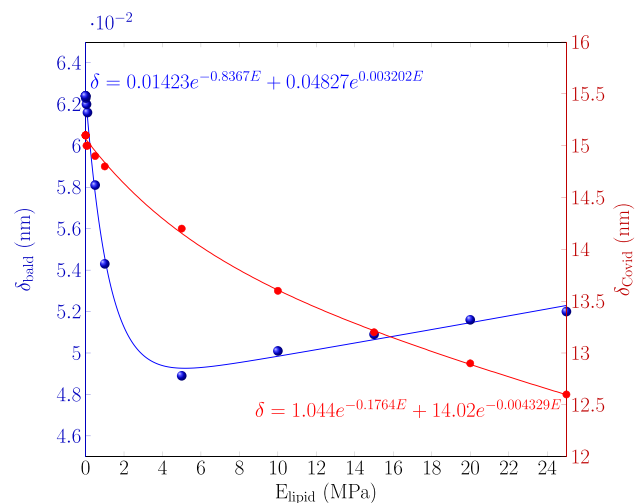
We can observe the exponential decay in both deformation and stress with the increase in the Young's modulus, and we can predict that the stiffness increases with the increase in Young's modulus as deformation and stiffness are inversely proportional to each other.

## 4 Discussion

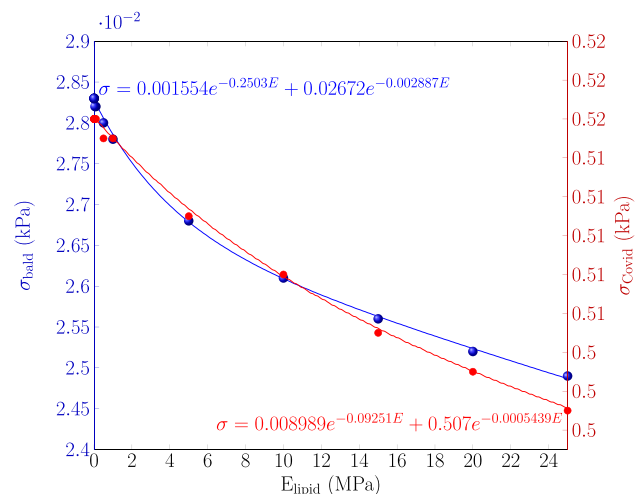
In recent years, various techniques were used to measure the mechanical response of the biological specimens. Atomic force microscopy has emerged as a technique to measure mechanical properties of the biological cells' on a nanoscale and yielded new insight to study their structural configuration's. In this study, numerical analysis was carried out to obtain the lipid and protein spike contribution to the mechanical stiffness of individual virions. The result shows that the mechanical response of untreated, native spiked COVID-19 was higher. COVID-19 shows maximum deformation and Vonmises Stress. This indicates a higher elastic behavior of COVID-19 compares to bald Virions. This leads to an increase in the flexibility of the COVID-19. There is a linear phase shown in the numerical analysis as it was shown by experimental results reported in the literature [36], which was approximately linear and highly reproducible. Consistent with this, bald virions' stiffness was higher than that of reconstituted COVID-19 of similar size. This difference may reflect a lower fluidity of the viral lipid bilayer and reinforcing effect of the membrane-associated proteins. In

bald virions, ectodomains of the glycoproteins are removed but possess the same structural arrangement. Due to the absence of the transmembrane part of the glycoproteins and M1 [3, 11] in bald virions leads to increase its stiffness. The stiffness of both viral models varies owing to material heterogeneity and spikes protruding beyond the membrane envelope's [36]. The stiffness of the various models was assessed throughout a diametrical range of nm, revealing a considerable difference between COVID-19 virus and bald virions. In contrast, bald virions were significantly stiffer over the entire range of particle size. This indicates that the influenza envelope's stiffness is determined by a combination of the stiffness of the lipid component and the membrane-associated viral protein components.

Furthermore, with the change in the geometrical and mechanical parameters of the COVID-19, we found the changes in the stiffness. In the bald virions, where there is



(a) Young's modulus vs deformation for bald virus and Covid-19



(b) Young's modulus vs stress for bald virus and Covid-19.

**Fig. 8** Variation in deformation and stress for bald and Covid-19



no interaction with the glycoprotein spikes, its mechanical behavior is different from that of the spike protruded viral structure. This suggests that the glycoproteins spike plays a vital role in the viral envelop while interacting with lipids and contributing to the change in the virions' mechanical behavior. Finite element modeling predicts the stiffness measured for the model systems (Covid-19 and bald virions) could be explained by the known physical properties of a viral envelop or a compact protein shell, as found for capsid-coated virus species. This numerical analysis significantly predicts the change in the stiffness values. The numerical findings differed from prior experimental results due to M1, which is near to the viral membrane, and frequent interactions between M1 and viral membrane constituents, especially HA and NA [5]. This numerical analysis shows no such behavior. Early experimental AFM literature anticipates a similar association to our results with minor volatility.

The impact of changing the thickness of the viral membrane and changing the envelop's Young's modulus on the virus's mechanical behavior was investigated in this work, and substantial alterations were estimated. On comparing the COVID-19 to bald virions, the contribution of spikes to the mechanical response of the COVID-19 was also determined.

## 5 Conclusion

Membrane with proteins capsid spike contributes to the mechanical properties of the virus particles. To interact and persist within the host cell, the COVID-19 virus requires flexibility in its envelope. It enable the dynamics in the host cell membrane during its viral life cycle, like receptor binding and viral fusion with the host cell and budding in case of viral assembly. We propose that these functions can be achieved by studying the dynamics of fluid that we consider as stable lipid bilayer in our present study and the effect of reinforced by membrane-associated proteins, including spike glycoproteins in the viral envelop. Even though the COVID-19 virions are unusually soft, but they can withstand larger deformations as we applied in our numerical analysis without showing much damage to the viral structure. This numerical study is constructive for studying the mechanical behavior of the COVID-19 and their comparison with the bald virions. We can conclude that the COVID-19 are softer and more elastic compared to bald virions from the study.

**Abbreviations** FE: finite element; SARS-CoV-2: severe acute respiratory syndrome coronavirus 2; MERS: Middle East respiratory syndrome; nCoV: novel corona virus; 3CLpro: 3-chymotrypsin like protease; DNA: deoxyribonucleic acid; AFM: atomic force microscopy; TMV: tobacco mosaic virus; RNA: ribonucleic acid; GPa: gigapascal; CAD: computer-aided design; HE: hemagglutinin esterase; RNP: ribonucleoprotein; HA: hemagglutinin; NA: neuraminidase; M1: influenza virus matrix protein

**Funding** This work is supported by additional competitive research grant BITS Pilani.

**Data Availability** The data that supports the findings of this study are available within the article.

## Declarations

**Informed Consent** There are no human subjects in this article and informed consent is not applicable.

**Conflict of Interest** The authors declare no competing interests.

## References

- Ahmed, R., Oldstone, M. B., & Palese, P. (2007). Protective immunity and susceptibility to infectious diseases: lessons from the 1918 influenza pandemic. *Nature Immunology*, *8*, 1188–1193.
- Bar-On, Y. M., Flamholz, A., Phillips, R., & Milo, R. (2020). Science forum: Sars-cov-2 (covid-19) by the numbers. *Elife*, *9*, e57309.
- Calder, L. J., Wasilewski, S., Berriman, J. A., & Rosenthal, P. B. (2010). Structural organization of a filamentous influenza A virus. *Proceedings of the National Academy of Sciences*, *107*, 10685–10690.
- Carrasco, C., Carreira, A., Schaap, I., Serena, P., Gomez-Herrero, J., Mateu, M., & De Pablo, P. (2006). Dna-mediated anisotropic mechanical reinforcement of a virus. *Proceedings of the National Academy of Sciences*, *103*, 13706–13711.
- Chen, B. J., Leser, G. P., Jackson, D., & Lamb, R. A. (2008). The influenza virus m2 protein cytoplasmic tail interacts with the m1 protein and influences virus assembly at the site of virus budding. *Journal of Virology*, *82*, 10059–10070.
- Falvo, M., Washburn, S., Superfine, R., Finch, M., Brooks, F., Jr., Chi, V., & Taylor, R., 2nd. (1997). Manipulation of individual viruses: friction and mechanical properties. *Biophysical Journal*, *72*, 1396–1403.
- Gallagher, T. M., & Buchmeier, M. J. (2001). Coronavirus spike proteins in viral entry and pathogenesis. *Virology*, *279*, 371–374.
- Gelderblom, H. R. (1996). Structure and classification of viruses. In *Medical Microbiology. 4th edition*. University of Texas Medical Branch at Galveston.
- Gittes, F., & Schmidt, C. F. (1998). Interference model for back-focal-plane displacement detection in optical tweezers. *Optics Letters*, *23*, 7–9.
- Gong, Z., Szczesny, S. E., Caliari, S. R., Charrier, E. E., Chaudhuri, O., Cao, X., et al. (2018). Matching material and cellular timescales maximizes cell spreading on viscoelastic substrates. *Proceedings of the National Academy of Sciences*, *115*, E2686–E2695.
- Harris, A., Cardone, G., Winkler, D. C., Heymann, J. B., Brecher, M., White, J. M., & Steven, A. C. (2006). Influenza virus pleiomorphy characterized by cryoelectron tomography. *Proceedings of the National Academy of Sciences*, *103*, 19123–19127.
- Ivanovska, I., De Pablo, P., Ibarra, B., Sgalari, G., MacKintosh, F., Carrascosa, J., et al. (2004). Bacteriophage capsids: tough nanoshells with complex elastic properties. *Proceedings of the National Academy of Sciences*, *101*, 7600–7605.
- Jadidi, T., Seyyed-Allaei, H., Tabar, M., & Mashaghi, A. (2014). Poisson's ratio and young's modulus of lipid bilayers in different phases. *Frontiers in Bioengineering and Biotechnology*, *2*, 8.

14. Jin, X., Lian, J.-S., Hu, J.-H., Gao, J., Zheng, L., Zhang, Y.-M., et al. (2020). Epidemiological, clinical and virological characteristics of 74 cases of coronavirus-infected disease 2019 (covid-19) with gastrointestinal symptoms. *Gut*, *69*, 1002–1009.
15. Khan, M. A., & Atangana, A. (2020). Modeling the dynamics of novel coronavirus (2019-ncov) with fractional derivative. *Alexandria Engineering Journal*.
16. Kim, J., Yoon, J.-C., & Kang, B.-S. (2007). Finite element analysis and modeling of structure with bolted joints. *Applied Mathematical Modelling*, *31*, 895–911.
17. Klein, S., Cortese, M., Winter, S. L., Wachsmuth-Melm, M., Neufeldt, C. J., Cerikan, B., et al. (2020). Sars-cov-2 structure and replication characterized by in situ cryo-electron tomography. *Nature Communications*, *11*, 1–10.
18. Kol, N., Shi, Y., Tsvitov, M., Barlam, D., Shneck, R. Z., Kay, M. S., & Rousso, I. (2007). A stiffness switch in human immunodeficiency virus. *Biophysical Journal*, *92*, 1777–1783.
19. Kuznetsov, Y., Gershon, P., & McPherson, A. (2008). Atomic force microscopy investigation of vaccinia virus structure. *Journal of Virology*, *82*, 7551–7566.
20. Kuznetsov, Y. G., Xiao, C., Sun, S., Raoult, D., Rossmann, M., & McPherson, A. (2010). Atomic force microscopy investigation of the giant mimivirus. *Virology*, *404*, 127–137.
21. Laue, M., Kauter, A., Hoffmann, T., Möller, L., Michel, J., & Nitsche, A. (2021). Morphometry of sars-cov and sars-cov-2 particles in ultrathin plastic sections of infected vero cell cultures. *Scientific Reports*, *11*, 1–11.
22. Laura, K., Peng, C., Jie, W., & Li Jie, P. (2020). Fighting the coronavirus outbreak. <https://pubs.acs.org/doi/pdf/10.1021/acscchembio.0c00175>.
23. Li, F. (2016). Structure, function, and evolution of coronavirus spike proteins. *Annual Review of Virology*, *3*, 237–261.
24. Li, S. (2012). *Atomic force microscopy study on the mechanics of influenza viruses and liposomes*. Ph.D. thesis Niedersächsische Staats-und Universitätsbibliothek Göttingen.
25. Li, X., Luk, H. K., Lau, S. K., & Woo, P. C. (2019). *Human coronaviruses: General features*. Reference Module in Biomedical Sciences, Elsevier. <https://doi.org/10.1016/B978-0-12-801238-3.95704-0>
26. Lin, S., Lee, C.-K., Lee, S.-Y., Kao, C.-L., Lin, C.-W., Wang, A.-B., et al. (2005). Surface ultrastructure of sars coronavirus revealed by atomic force microscopy. *Cellular Microbiology*, *7*, 1763–1770.
27. Lu, H., Stratton, C. W., & Tang, Y.-W. (2020). Outbreak of pneumonia of unknown etiology in wuhan china: the mystery and the miracle. *Journal of Medical Virology*, *92*(4), 401–402. <https://doi.org/10.1002/jmv.25678>.
28. Mateu, M. G. (2012). Mechanical properties of viruses analyzed by atomic force microscopy: a virological perspective. *Virus Research*, *168*, 1–22.
29. Michel, J., Ivanovska, I., Gibbons, M., Klug, W., Knobler, C., Wuite, G., & Schmidt, C. (2006). Nanoindentation studies of full and empty viral capsids and the effects of capsid protein mutations on elasticity and strength. *Proceedings of the National Academy of Sciences*, *103*, 6184–6189.
30. Moffitt, J. R., Chemla, Y. R., Athavan, K., Grimes, S., Jardine, P. J., Anderson, D. L., & Bustamante, C. (2009). Intersubunit coordination in a homomeric ring atpase. *Nature*, *457*, 446–450.
31. Momeni Bashusqeh, S., & Rastgoo, A. (2016). Elastic modulus of free-standing lipid bilayer. *Soft Materials*, *14*, 210–216.
32. Rawicz, W., Olbrich, K. C., McIntosh, T., Needham, D., & Evans, E. (2000). Effect of chain length and unsaturation on elasticity of lipid bilayers. *Biophysical Journal*, *79*, 328–339.
33. Roos, W., Ivanovska, I., Evilevitch, A., & Wuite, G. (2007). Viral capsids: mechanical characteristics, genome packaging and delivery mechanisms. *Cellular and molecular life sciences*, *64*, 1484.
34. Roos, W. H., Gertsman, I., May, E. R., Brooks, C. L., Johnson, J. E., & Wuite, G. J. (2012). Mechanics of bacteriophage maturation. *Proceedings of the National Academy of Sciences*, *109*, 2342–2347.
35. Roos, W. H., Radtke, K., Kniesmeijer, E., Geertsema, H., Sodeik, B., & Wuite, G. J. (2009). Scaffold expulsion and genome packaging trigger stabilization of herpes simplex virus capsids. *Proceedings of the National Academy of Sciences*, *106*, 9673–9678.
36. Schaap, I. A., Eghiaian, F., des Georges, A., & Veigel, C. (2012). Effect of envelope proteins on the mechanical properties of influenza virus. *Journal of Biological Chemistry*, *287*, 41078–41088.
37. Smith, D. E., Tans, S. J., Smith, S. B., Grimes, S., Anderson, D. L., & Bustamante, C. (2001). The bacteriophage  $\phi$ 29 portal motor can package dna against a large internal force. *Nature*, *413*, 748–752.
38. Stephanidis, B., Adichtchev, S., Gouet, P., McPherson, A., & Mermet, A. (2007). Elastic properties of viruses. *Biophysical Journal*, *93*, 1354–1359.
39. Stoermer, M. (2020). Homology models of coronavirus 2019-ncov 3clpro protease. *chemrxiv*.